

Actinide solubility-controlling phases during the dissolution of phosphate ceramics

E. Du Fou de Kerdaniel ^a, N. Clavier ^a, N. Dacheux ^{a,*}, O. Terra ^a, R. Podor ^b

^a *Groupe de Radiochimie, IPNO, Université Paris-Sud-11, 91406 Orsay, France*

^b *Laboratoire de Chimie du Solide Minéral, Université H. Poincaré – Nancy I, BP 239, 54506 Vandoeuvre lès Nancy, France*

Abstract

Phosphate ceramics (britholites, monazite/brabantite solid solutions, thorium phosphate diphosphate, i.e. β -TPD, and associated β -TPD/monazite composites) are often considered as potential candidates to immobilize tri- and tetravalent actinides. In order to study the properties of such materials on the retention of actinides during aqueous alteration, phosphate-based neoformed phases were prepared using under- and over-saturation processes then extensively characterized (involving grazing XRD, EPMA, μ -Raman, IR or SEM). In over-saturation conditions, lanthanides (used as surrogates of trivalent actinides) are quickly precipitated as three hydrated forms (monazite, rhabdophane or xenotime) depending on the temperature, the heating time and the ionic radius of the element. Moreover, as already described for thorium, tetravalent actinides (Th, U, Np, Pu) are more often immobilized as phosphate hydrogenphosphate compounds. However, samples of (Ln,Ca,Th)-rhabdophane can also precipitate in the presence of large concentrations of calcium. Such neoformed phases were also precipitated at the surface of leached phosphate-based ceramics during under-saturation experiments. The associated thermodynamic solubility constants at infinite dilution were estimated. Due to their rapid precipitation and their very low solubility constants, these actinide phosphate solubility-controlling phases appear of significant interest in the field of the evaluation of the long-term performance of actinide-doped phosphate ceramics.

© 2007 Elsevier B.V. All rights reserved.

1. Introduction

Several phosphate-based ceramics such as britholite $\text{Ca}_9\text{Nd}_{1-x}\text{An}_x^{\text{IV}}(\text{PO}_4)_{5-x}(\text{SiO}_4)_{1+x}\text{F}_2$, monazite/brabantite solid solutions $\text{Ca}_x\text{Ln}_{1-x}\text{An}_x^{\text{IV}}\text{PO}_4$, thorium phosphate diphosphate (β - $\text{Th}_4(\text{PO}_4)_4\text{P}_2\text{O}_7$) and associated β -TPD/Monazite composites were already proposed as potential candidates for the long-term specific immobilization of actinides [1,2].

For each material, the incorporation of thorium, uranium(IV) and lanthanides (used as trivalent actinides surrogates) was examined through dry chemistry routes based on successive cycles combining mechanical grinding and heating treatment at high temperature (1373–1673 K) [3] or through wet chemistry methods from solutions or powdered crystallized low-temperature precursors [4]. In order to guarantee the efficient immobilization of actinides, several physico-chemical properties such as high loading capability, good properties of sintering or good resistance to radiation damage are required [5].

* Corresponding author. Tel.: + 33 1 69 15 73 46; fax: + 33 1 69 15 71 50.

E-mail address: dacheux@ipno.in2p3.fr (N. Dacheux).

The last main property of interest required deals with the chemical durability of the synthesized materials near and far from saturation processes. Consequently, the behavior of the ceramics loaded with actinides or with surrogate elements was examined through a dual approach combining kinetics (multiparametric expression of the normalized dissolution rates) and thermodynamics (identification/characterization of neoformed phases then estimation of the associated solubility constants). In this field, the retention of these actinides during aqueous alteration was studied either by making leaching tests of sintered pellets in aggressive media (called ‘under-saturation’ experiments) or by studying the solubility-controlling neoformed phases through their precipitation in over-saturation conditions.

2. Experimental

2.1. Synthesis and characterization of the initial ceramics

The phosphate-based ceramics containing tetravalent actinides (Th, U) or trivalent lanthanides (used as surrogates of actinides) were prepared through dry chemistry routes using mechanical grinding of the initial mixtures followed by heating at high temperature (1373–1673 K) or wet chemistry methods from a mixture of concentrated solutions or from low-temperature crystallized precursors [3,4]. We checked through an extensive characterization including grazing XRD, spectroscopic techniques (infrared, μ -Raman, . . .), scanning electron microscope observations (SEM) and electron probe microanalyses (EPMA), that all the final ceramics were single phase and homogeneous, leading to the preparation of solid solutions with the expected chemical composition [3].

2.2. Leaching tests (under-saturation experiments)

The resistance of the prepared materials to aqueous alteration was evaluated through leaching tests performed in high density polyethylene (HDPE) or polytetrafluoroethylene (PTFE) containers with low or high leachate renewal (called ‘static’ or ‘dynamic’ experiments, respectively). The elementary concentrations were determined by inductively coupled plasma-mass spectroscopy (ICP-MS), α -scintillation technique or time-resolved laser fluorescence spectroscopy (TRLFS) for several leaching

times. The normalized dissolution rate R_L ($\text{g m}^{-2} \text{d}^{-1}$) which represents the mass loss of the dissolved solid per time and surface units, was determined from the normalized leachings, N_L (g m^{-2}), according to the following equation [6]:

$$R_L(i) = \frac{dN_L(i)}{dt} = \frac{d}{dt} \left(\frac{C_i \times V \times M_i}{x_i \times S} \right), \quad (1)$$

where C_i represents the concentration of the measured element, V the volume of the leachate, x_i the mass ratio of the element i in the solid, M_i the molar mass of i and S the effective surface area of the pellet.

2.3. Preparation and characterization of actinides solubility – controlling neoformed phases (over-saturation experiments)

Wet chemistry methods involving stoichiometric mixtures of acidic solutions containing the cations (An, Ln) and 5 M H_3PO_4 were performed to prepare the actinides solubility-controlling neoformed phases (an excess of 2 mol.% of H_3PO_4 being considered to ensure the quantitative precipitation of the cations). The mixtures were placed in PTFE closed containers then heated on a sand bath or in autoclaves for few hours to several months. During this step, the gels initially formed (especially when using tetravalent elements) progressively turned into crystallized precipitates. The solids obtained were separated from the supernatant by centrifugation at 3500 rpm, washed several times with deionized water then ethanol, dried, ground and finally characterized. The associated precipitation yields, ρ , varied from 60–67% (1 M HCl or HNO_3) to $84 \pm 5\%$ (10^{-1} M HCl) for trivalent elements while the precipitation of tetravalent actinides was always quantitative ($99.2\% \leq \rho \leq 99.9\%$) for all the acidic media considered.

3. Results and discussion

3.1. Description of the ceramics behaviour during dissolution

The evolution of the normalized leachings is reported in Fig. 1 for several phosphate-based ceramics ((Nd,Th)-britholite, (Th,U)-monazite/bra-bantite, β -TUPD and β -TUPD/monazite composites). For all the samples, the congruent part of the dissolution initially observed during the first days of leaching tests is rapidly followed by an

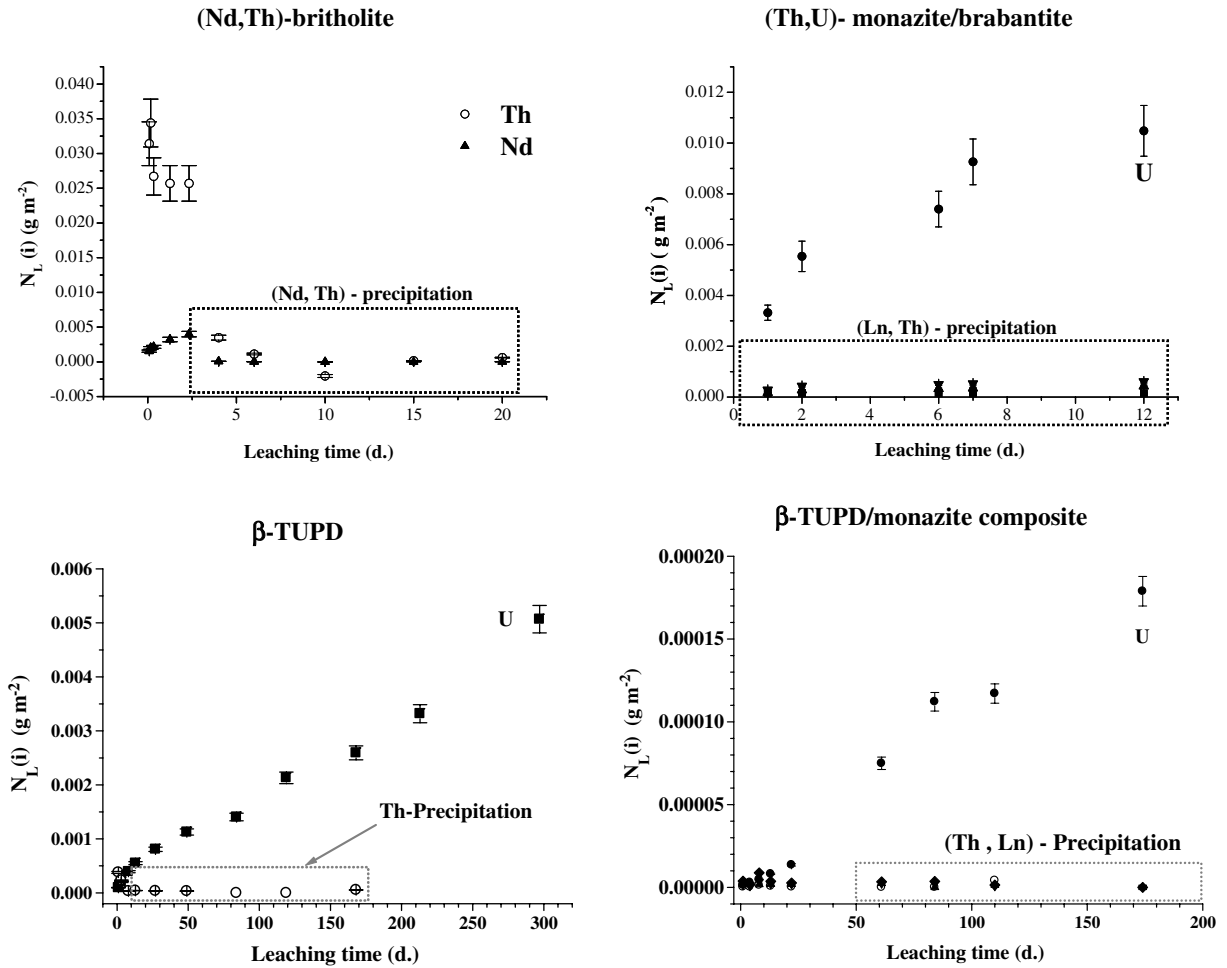


Fig. 1. Evolution of normalized leachings, $N_L(i)$, obtained when leaching phosphate-based materials: (Nd,Th)-britholite (○: Th, ▲: Nd), (Th,U)-monazite/brabantite solid solutions (◆: Th, ▼: Ln, ●: U), β -TUPD (○: Th, ■: U) and β -TUPD/Gd-monzite composite (◆: Th, ●: U, ○: Ln) in 10^{-1} M HNO_3 at 363 K.

incongruent step in static conditions, consequently to the formation of thorium and/or lanthanides bearing neoformed phosphates onto the surface of the pellets or inside amorphous layers. This phenomenon was partly avoided by making dynamic experiments in 10^{-1} M HNO_3 (with high leaching flow rates), leading to the accurate determination of the normalized dissolution rate values. Using this method, the $R_L(i)$ values ranged from 10^{-7} $\text{g m}^{-2} \text{d}^{-1}$ to 10^{-3} $\text{g m}^{-2} \text{d}^{-1}$ which appears very low compared to materials such as basaltic glasses and in good agreement with the data reported in the literature for natural analogues [7].

After this first step, a strong decrease of $R_L(\text{Th})$ and $R_L(\text{Ln})$ is observed consequently to their involvement in the formation of neoformed phases. However, the elementary releases being very low,

the complete characterization of these actinide solubility-controlling phases was complicated by the small amount of precipitated solids onto the surface of the leached samples. For this reason, the characterization of such phases was first reached indirectly by making over-saturation experiments then correlated to the data obtained during the dissolution of ceramics.

3.2. Identification of neoformed phases in over-saturation experiments

For trivalent elements, the nature of the precipitated phases was followed versus several parameters (ionic radius: r_C , heating temperature, heating time, cation concentrations,...). For instance, for $T = 423$ K, one week of heating time and

$0.01 \text{ M} \leq C_M \leq 0.5 \text{ M}$, the nature of the neoformed phase $\text{LnPO}_4 \cdot n\text{H}_2\text{O}$ strongly depends on the ionic radius of the lanthanide element. Indeed, the monazite structure (monoclinic system, $P_{21/n}$, coordination number $\text{CN} = \text{IX}$) is precipitated for light lanthanides (La–Ce, $0.116 \text{ nm} \geq r_C \geq 0.114 \text{ nm}$), rhabdophane structure (hexagonal system, P_{3121} , $\text{CN} = \text{VIII}$) from neodymium to dysprosium ($0.111 \text{ nm} \geq$

$r_C \geq 0.103 \text{ nm}$) and xenotime structure (quadratic system, I_{41amd} , $\text{CN} = \text{VIII}$) for heavy lanthanides (Ho–Lu, $0.102 \text{ nm} \geq r_C \geq 0.098 \text{ nm}$). When extending the study to other temperatures (Figs. 2–4, Table 1), monazite is clearly formed for the higher temperatures considered (typically above 433 K for all the lanthanide considered) while rhabdophane appears as a ‘low-temperature’ phase. This later

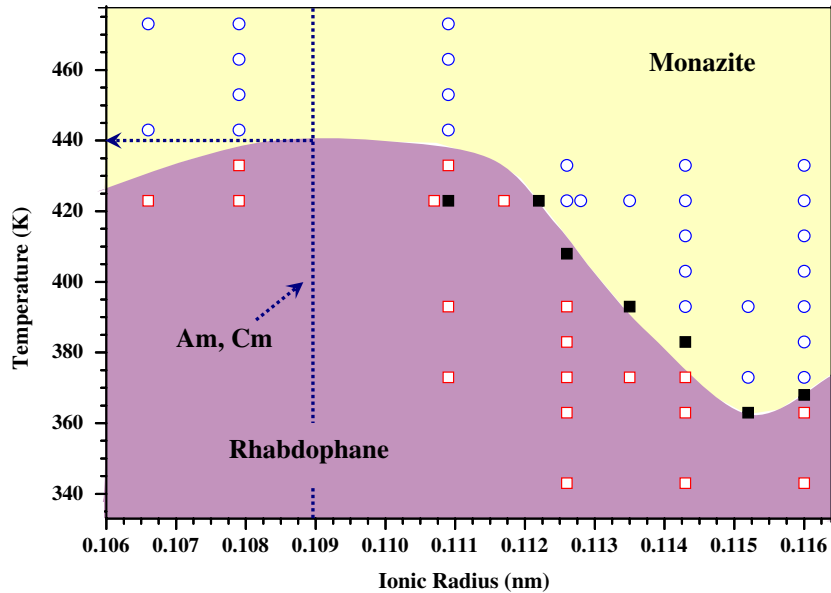


Fig. 2. Nature of the precipitated lanthanide phosphate versus the heating temperature and the ionic radius of the lanthanide element (○: monazite; □: rhabdophane; ■: mixture of monazite and rhabdophane).

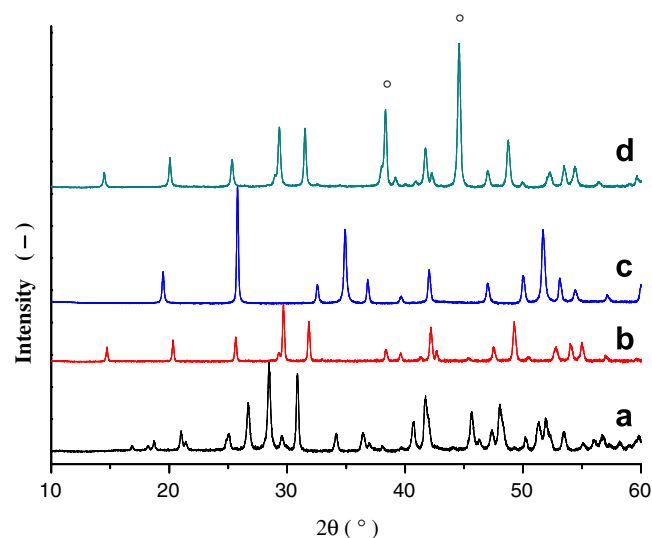


Fig. 3. XRD diagrams of precipitated La-monazite ($T = 383 \text{ K}$) (a), Sm-rhabdophane ($T = 393 \text{ K}$) (b), Er-xenotime ($T = 423 \text{ K}$) (c) and (La,Ca,Th)-rhabdophane ($T = 423 \text{ K}$, $t = 27 \text{ days}$) (d). ○: XRD peaks of the holder.

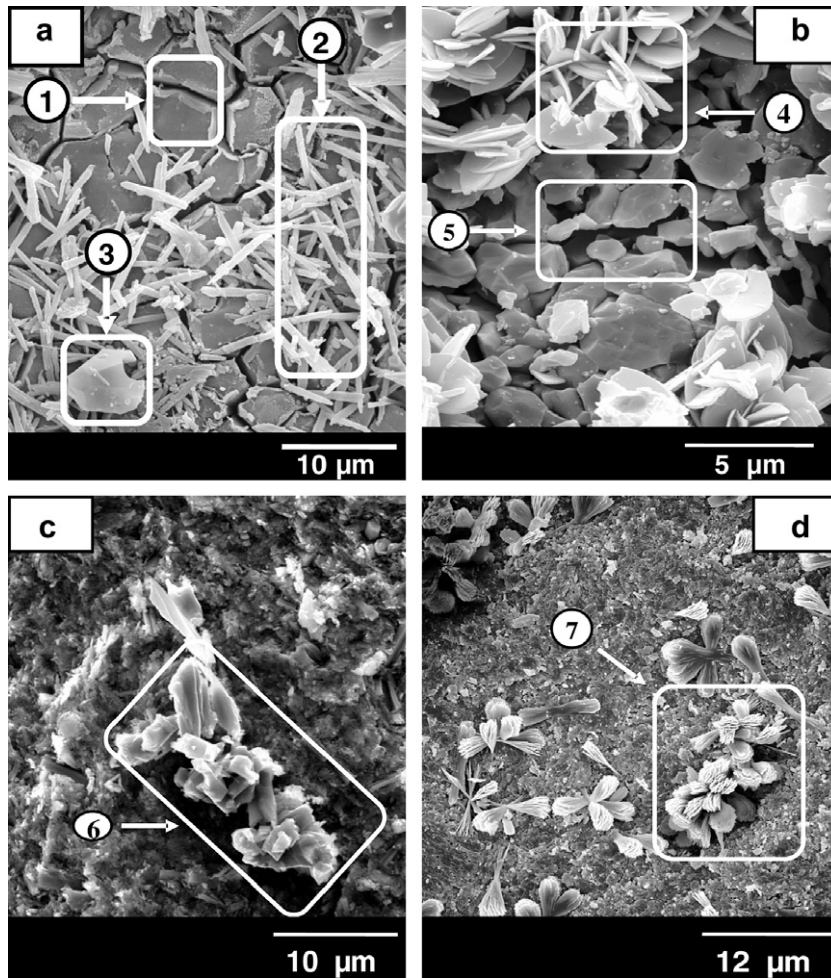


Fig. 4. SEM observation of leached (Nd,Th)-britholite (a), β-TUPD (b) and β-TUPD/Ln-monazite composites (c and d) showing the precipitation of $\text{Ca}_x\text{Nd}_{1-2x}\text{Th}_x\text{PO}_4 \cdot 1/2 \text{H}_2\text{O}$ (2), $\text{SiO}_2 \cdot n \text{H}_2\text{O}$ (3), T(U)PPPH (4,7) and Gd-rhabdophane (6).

Table 1

Lanthanide containing neoformed phases (La, Ce, Pr) formed in over-saturation conditions for several temperatures of synthesis ($t = 1$ week)

| T (K) | 343 | 363 | 373 | 383 | 393 | 403 | 413 | 423 | 433 |
|--------------|-------|-------|-------|-------|-------|------|------|------|------|
| Lanthanum | Rhab. | Rhab. | Mon. | Mon. | Mon. | Mon. | Mon. | Mon. | Mon. |
| Cerium | Rhab. | Rhab. | Rhab. | Mix. | Mon. | Mon. | Mon. | Mon. | Mon. |
| Praseodymium | Rhab. | Rhab. | Rhab. | Rhab. | Rhab. | Mix. | Mix. | Mon. | Mon. |

Rhab.: rhabdophane; Mon.: monazite; and Mix: mixture of rhabdophane and monazite.

point can be also correlated to literature coming from geochemical observations in which monazite is often observed while rhabdophane phases appear more rarely. On this basis, both structures could be formed when dissolving the initial ceramics in our experimental conditions of leaching ($298 \text{ K} \leq T \leq 433 \text{ K}$). Moreover, considering the

ionic radii of trivalent americium and curium ($r_C = 0.109 \text{ nm}$ for $\text{CN} = \text{VIII}$), the rhabdophane should be formed below 440 K while monazite would be precipitated above this temperature (Fig. 2). These results appear in good agreement with that reported by Keller and Walter [8] who precipitated well crystallized hexagonal Am-rhabdophane sam-

ples ($a = 0.699$ nm and $c = 0.639$ nm) from a mixture of Na_2HPO_4 and Am(III) solution after making hydrothermal synthesis at 423 K and reported the transformation into the Am-monazite above 473 K.

Contrarily to trivalent elements, the behaviour of tetravalent actinides during leaching tests was already described [9]. Indeed, tetravalent thorium and uranium (under anoxic conditions) usually precipitate as the low-soluble actinide phosphate hydrogenphosphate hydrates of formula $\text{An}_{x/2}\text{-Th}_{2-x/2}(\text{PO}_4)_2(\text{HPO}_4) \cdot \text{H}_2\text{O}$ [4,9]. Other experiments showed that tetravalent plutonium and neptunium behave the same way [10]. However, since calcium could participate with phosphate groups to the formation of other neoformed phases, the behaviour of tetravalent actinides was also studied in the presence of large calcium concentration. Using this method, the formation of an unknown rhabdophane-type compound of formula $\text{Ca}_{0.1}\text{-Nd}_{0.8}\text{Th}_{0.1}\text{PO}_4 \cdot 1/2 \text{H}_2\text{O}$ (EPMA results: 12.9 wt% (P); 1.5 wt% (Ca); 48.2 wt% (Nd) and 10.6 wt% (Th)) was observed. The refined unit-cell parameters ($a = 0.7012(3)$ nm and $c = 0.6402(3)$ nm) are in good agreement with that reported for $\text{NdPO}_4 \cdot 1/2 \text{H}_2\text{O}$ ($a = 0.7014(3)$ nm and $c = 0.6401(4)$ nm) [11] and confirmed the incorporation of calcium and thorium in the structure. The kinetic stability of such a phase was thus followed versus the heating time. From the EPMA results, it appeared that the thorium weight percent decreases progressively down to 7.5 wt% after 27 days and to 6.4 wt% after two months, correlatively to the increase of the neodymium weight loading. Simultaneously, the XRD analysis revealed the progressive formation of $\text{Th}_2(\text{PO}_4)_2(\text{HPO}_4) \cdot \text{H}_2\text{O}$ (TPHPH). Both observations appear consistent with the conclusions given by Jonasson et al. when studying the solubilities of some hydrated rare-earth phosphates with implications for diagenesis and sea water concentrations [12]. In this work, the authors suggest that hydrated phosphates are important phases in controlling the sea water rare-earth concentrations. However, they also noted that the relationship between rhabdophane and monazite is not clear but that rhabdophane could be considered as a meta-stable phase compared to monazite. Consequently, the existence of rhabdophane could result from a greater precipitation rate while monazite should be more difficult to dissolve but also to precipitate from ions in solution. These observations on natural analogues were also confirmed on our samples by leaching La-rhabdophane and La-monazite in the conditions of sta-

bility of La-monazite (1 M HCl, $T = 393$ K) and La-rhabdophane (1 M HCl, $T = 363$ K), respectively. With this approach, we observed the slow transformation of La-rhabdophane into La-monazite but, inversely, no modification of the La-monazite sample.

3.3. Analysis of the leached samples during saturation processes

In order to reach the saturation conditions through under-saturation experiments, sintered samples of the phosphate-based ceramics were leached for several months in aggressive media which led to the precipitation of neoformed phases at the solid/liquid interface. SEM observations and grazing XRD diagrams are given in Figs. 4 and 5, respectively, while EPMA results are reported in Table 2 for leached (Nd,Th)-britholites. From these data, the presence of neoformed phases is confirmed onto the surface of the leached pellets for all the solids considered. Moreover, the SEM micrographs suggest a scheme of dissolution based on the following successive steps: reaction inside the grain boundaries and break away of the grains (① and ⑤ in Fig. 4 on leached (Nd,Th)-britholite or β -TUPD) associated to the release of elements in the leachate then formation of gelatinous or crystallized neoformed phases ((②-④,⑥,⑦ in Fig. 4). From EPMA results, especially considering the $(\text{Ca} + \text{Th})/\text{Nd}$ and $(\text{Ca} + \text{Th} + \text{Nd})/\text{P}$ mole ratios, and from grazing XRD, the needle like crystals precipitated onto the surface of leached (Nd,Th)-britholite are identified to the $\text{Ca}_x\text{Nd}_{1-2x}\text{Th}_x\text{PO}_4 \cdot 1/2 \text{H}_2\text{O}$ rhabdophane (②). This phase coexists with amorphous hydrated silica $\text{SiO}_2 \cdot n\text{H}_2\text{O}$ (③) while the bulk of the material remains almost unchanged. For leached β -TUPD and associated β -TUPD/monazite composites, circular plate-like crystals of uranium depleted T(U)PHPH , $\text{U}_{x/2}\text{Th}_{2-x/2}(\text{PO}_4)_2(\text{HPO}_4) \cdot \text{H}_2\text{O}$ (④,⑦), and bigger aggregates of 10–15 μm in length, are observed while for the latter material needle like crystals of Gd-rhabdophane (⑥) are also observed. It is worth to note that several neoformed phases are common to the various ceramics studied whatever the leaching conditions considered.

In order to evaluate the contribution of such precipitates to the long-term retention of actinides, the associated solubility constants were estimated at infinite dilution from the elementary concentrations at equilibrium (Table 3, [12–17]) considering the Specific Interaction Theory. All the values obtained

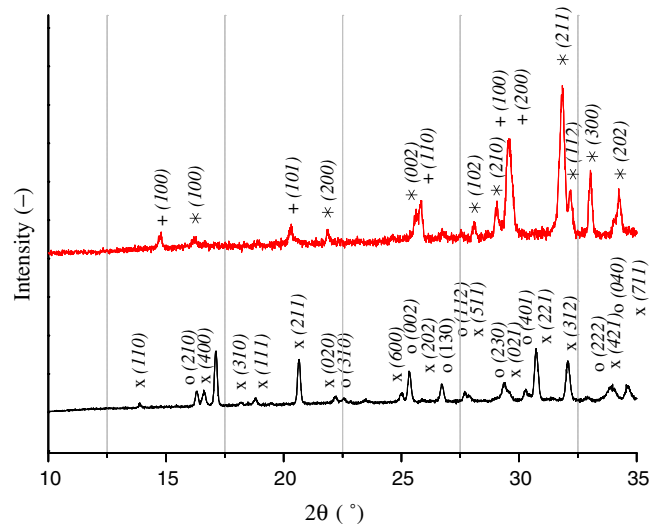


Fig. 5. Characterization of leached (Nd, Th)-britholite (up) or β -TUPD (down) by grazing XRD. XRD lines of (Nd,Th)-britholite (*), (Nd,Ca,Th)-rhabdophane (+), β -TUPD (○) and T(U)PPH (×).

Table 2
EPMA results obtained during the dissolution of (Nd,Th)-britholite (under-saturation experiments)

| Weight fraction (%) | O | F | Si | P | Ca | Nd | Th | Cation/P |
|-------------------------|------------|-----------|------------|------------|------------|------------|------------|----------|
| ① | 34.9 ± 0.2 | 1.8 ± 0.2 | 3.6 ± 0.1 | 12.2 ± 0.3 | 30.4 ± 0.1 | 6.3 ± 0.4 | 10.5 ± 0.7 | – |
| ② | 27.4 ± 1.4 | 1.2 ± 0.9 | 0.6 ± 1.0 | 13.1 ± 0.5 | 4.5 ± 0.2 | 30.8 ± 1.4 | 21.8 ± 2.0 | 0.99 |
| ② | 27.1 ± 0.3 | 1.0 ± 0.1 | 0.1 ± 0.1 | 13.2 ± 0.1 | 5.9 ± 0.3 | 19.4 ± 0.6 | 32.8 ± 0.9 | 1.00 |
| ③ | 55.9 ± 5.8 | 0.5 ± 0.1 | 38.2 ± 5.5 | 0.6 ± 0.9 | 0.5 ± 0.2 | 1.5 ± 2.2 | 2.5 ± 0.2 | – |
| Calculated ^a | 33.5 | 3.3 | 3.7 | 12.1 | 31.3 | 6.3 | 10.1 | – |

^a Calculated on the basis of the (Nd,Th)-britholite formula.

Table 3
Values of $\log(K_{S,0}^{\circ})$ obtained (reported) for some actinide and lanthanide phosphates

| Compound | $\log(K_{S,0}^{\circ})$ | T (K) | Ref. |
|--|-------------------------|---------|----------------------|
| $\text{Th}_2(\text{PO}_4)_2(\text{HPO}_4) \cdot \text{H}_2\text{O}$ | -66.6 ± 1.1 | 298 | [13] ^a |
| $\text{Pu}_{x/2}\text{Th}_{2-x/2}(\text{PO}_4)_2(\text{HPO}_4) \cdot \text{H}_2\text{O}$ | -63.2 ± 1.1 | 298 | [15] ^a |
| $\text{LaPO}_4 \cdot 1/2 \text{H}_2\text{O}$ (rhabdophane) | $-24.5, -27.4$ | 298 | [12,13] ^a |
| $\text{NdPO}_4 \cdot 1/2 \text{H}_2\text{O}, \text{PrPO}_4 \cdot 1/2 \text{H}_2\text{O}$ (rhabdophane) | $-26.0, -25.7$ | 373 | [12,14] ^a |
| $\text{ErPO}_4 \cdot n \text{H}_2\text{O}$ (xenotime) | -25.5 | 373 | [12] |
| $\text{AmPO}_4 \cdot n \text{H}_2\text{O}$ | $-24.8, -27.2 \pm 0.5$ | 298 | [16,15] |
| $\text{CmPO}_4 \cdot n \text{H}_2\text{O}$ | -29.2 ± 0.4 | 298 | [15] |
| $\text{Ca}_{0.1}\text{Nd}_{0.8}\text{Th}_{0.1}\text{PO}_4 \cdot 1/2 \text{H}_2\text{O}$ | <i>Work in progress</i> | | |
| $(\text{UO}_2)_3(\text{PO}_4)_2 \cdot 5 \text{H}_2\text{O}$ | $-55.1 / -53.3$ | 298 | [16,17] |

^a This work.

are characteristic of very low-soluble phases which confirms the significant role they could play in the field of the immobilization of actinides in phosphate ceramics. The complete discussion in the evaluation of these associated thermodynamic data ($\Delta_R H^{\circ}$, $\Delta_R S^{\circ}$, $K_S^{\circ}(T)$, ...), necessary for the long-term behaviour assessment, will be discussed soon espe-

cially for tetravalent actinides bearing phosphate precipitates.

4. Conclusions

The results obtained from under- and over-saturation experiments exhibited various actinide

behaviours during the dissolution of phosphate or phosphate–silicate based ceramics, depending on their redox properties. Indeed, whatever the nature of the ceramic, trivalent elements are usually precipitated as rhabdophane-type solids that ensure their rapid retention. However, these solids can be transformed by increasing the leaching temperature and lead to the more stable monazite compounds which confers to this latter the bigger role for long-term retention considerations. The behaviour of actinides stabilized in the tetravalent oxidation state usually follows that of thorium through their quantitative precipitation as TPHPH-type solids. Even though the formation of (Ln,Ca,Th)-rhabdophane can be also reported in presence of large concentrations of calcium, its progressive transformation into TPHPH seems to confirm the thermodynamic meta-stability of rhabdophanes. Finally, while the behaviour of thorium, americium or curium can thus be predicted through their involvement in such neoformed phases, that of plutonium or neptunium could be more difficult to evaluate because of their potential stabilization in several oxidation states. Indeed, in their tetravalent form, they would certainly form TAn^{IV}PHPH compounds, like uranium, as checked by over-saturation experiments. For other oxidation states, they could form additional unknown neoformed phases. In these conditions, the chemical behaviour of these elements must be studied carefully, like for uranium which was found to precipitate as the uranyl phosphate pentahydrate when leaching β -TUPD or β -TUPD/monazite samples in oxidizing conditions.

Acknowledgements

This work was financially and scientifically supported by the French research program NOMADE (CNRS/CEA/COGEMA: GdR 2023) and by the ACTINET european network (workpackage JRP02-28). The authors are grateful to J. Ravaux, A. Kolher and T. Lhomme from LCSM and CRE-

GU from university Henri Poincaré of Nancy (France) for their contribution in the EPMA analyses, the SEM observations and the μ -Raman characterizations.

References

- [1] X. Deschanel, Evaluation de la faisabilité technique des nouvelles matrices de conditionnement des radionucléides à vie longue, Technical report CEA, DTCD/2004/5, 2004.
- [2] N. Dacheux, N. Clavier, A.C. Robisson, O. Terra, F. Audubert, J.E. Lartigue, C. Guy, C. R. *Chimie* 7 (2004) 1141.
- [3] O. Terra, N. Dacheux, F. Audubert, R. Podor, J. Nucl. Mater. 352 (2006) 224.
- [4] N. Clavier, N. Dacheux, G. Wallez, M. Quarton, J. Nucl. Mater. 352 (2006) 209.
- [5] C. Tamain, A. Özgümüş, N. Dacheux, F. Garrido, L. Thomé, J. Nucl. Mater. 352 (2006) 217.
- [6] N. Dacheux, N. Clavier, J. Ritt, J. Nucl. Mater. 349 (2006) 291.
- [7] E.H. Oelkers, F. Poitrasson, *Chem. Geol.* 73 (2002) 191.
- [8] C. Keller, K.H. Walter, *J. Inorg. Nucl. Chem.* 27 (1965) 1253.
- [9] N. Clavier, E. Du Fou de Kerdaniel, N. Dacheux, P. Le Coustumer, R. Drot, J. Ravaux, E. Simoni, J. Nucl. Mater. 349 (2006) 304.
- [10] J. Rousselle, Etude de la formation du phosphate diphosphate de thorium (PDT) en milieu nitrique en vue d'une décontamination d'effluents de haute activité contenant des actinides, PhD thesis, Université Paris-Sud-11, IPNO-T-04.03, 2004.
- [11] O. Terra, N. Clavier, N. Dacheux, R. Podor, *New J. Chem.* 27 (2003) 957.
- [12] R.G. Jonasson, G.M. Bancroft, H.W. Nesbitt, *Geochim. Cosmochim. Acta* 49 (1985) 2133.
- [13] N. Clavier, Elaboration de phosphate–diphosphate de thorium et d'uranium (β -PDTU) et de matériaux composites β -PDTU/monazite à partir de précurseurs cristallisés, Etudes du frittage et de la durabilité chimique, PhD thesis, Université Paris-Sud-11, IPNO-T-04.15, 2004.
- [14] F. Poitrasson, E.H. Oelkers, J. Schott, J.M. Montel, *Geochim. Cosmochim. Acta* 68 (2004) 2207.
- [15] A.C. Robisson, N. Dacheux, J. Aupiais, *J. Nucl. Mater.* 306 (2002) 134.
- [16] D. Rai, A.R. Felmy, R.W. Fulton, *Radiochim. Acta* 56 (1992) 7.
- [17] A.C. Thomas, N. Dacheux, P. Le Coustumer, V. Brandel, M. Genet, *J. Nucl. Mater.* 295 (2001) 249.